Development of a Simulator for Laboratory HVAC System

Authors:
Osman Ahmed, Ph.D., P.E.
Landis & Staefa
Buffalo Grove, IL 60089, USA

Prof. J.W. Mitchell, Ph.D., P.E.
University of Wisconsin- Madison
Madison, WI 53706

Prof. S.A. Klein, Ph.D.
Address same as above

ABSTRACT:

Space conditioning of a laboratory environment is more complicated than that of a typical commercial office building space. Safety considerations impose additional constraints over the usual comfort requirements. The control actions required to provide safety often counteracts those needed to meet comfort criteria. The dynamic interaction between the different control systems is complex and critical to laboratory safety.

A description of a dynamic simulator for use in design and evaluation of laboratory HVAC systems is presented in this paper. The simulator includes the laboratory envelope, air flow system, heating and cooling coils, and a proportional-integral controller. The simulator is based on physical mechanisms and generates the transient response of the controlled variables (i. e. room temperature and pressure differential) to forcing functions (e.g. thermal loads, exhaust flows). The controller incorporates a model-based predictor that provides a rapid response to maintain comfort in the space while at the same time meeting safety criteria.

The dynamic response of the pressure differential control and temperature control for both heating and cooling are important to energy use and safety in a laboratory environment. Significant changes in air flow rates and loads occur rapidly and tolerances are small. Results using the simulator are presented for the common control sequences found in a variable air volume (VAV) laboratory system. The simulator is found to be a promising approach to designing the control systems for a laboratory environment. The simulator provides insight into the dynamic interaction of the different control systems and the response of the laboratory environment. The simulator may serve as a model for developing the next generation of laboratory controllers.

INTRODUCTION:

This paper focuses on developing a complete simulation model to represent the laboratory thermal environment, the associated HVAC and control systems. The need for such a simulator in studying both steady and transient response of laboratory environment during the design process is critical. In order to develop and test new control strategies for a laboratory, a simulator can be used as a test bed to analyze the performance of the laboratory and HVAC systems. With the use of an simulator, the risk of applying an unproven control strategy in a real laboratory environment is eliminated. A simulator provides a cost effective approach to test and compare different control strategies. This

paper describes the development of an simulator in terms of the governing mathematical models, underlying assumptions, significance and boundary constraints. The simulator replicates the behavior of a laboratory environment and associated HVAC and control systems.

The modeling and simulation of a room environment and its associated HVAC and control systems has focused primarily on commercial space (Athienitis et al. 1990; Borrenson 1981; Li and Wepfer 1987; Mehta 1987; Park et al. 1989; Zaheer-uddin and Zheng 1994). The main objective in these studies was to investigate the impact of the space thermal conditions on energy use and comfort. Similar studies for a laboratory space, however, are scarce. The laboratory environment is unique compared to a commercial space in that safety constraints are added to those for comfort and energy. The laboratory operating condition often changes rapidly due to fume hood exhaust flows and laboratory equipment load. The dynamic pressure changes are often large. The uniqueness of laboratory environment is well documented (ASHRAE 1995; Neuman 1989). Shah (1980) used conservation of mass and leakage equations to estimate the time required to increase or decrease the space pressure. Anderson (1987) presented a theoretical analysis to define control requirements on space pressurization. Mass, energy and leakage equations were simultaneously solved to study the laboratory space dynamic response by Ahmed et al. (1993). The change in air density was considered in the analysis. Ahmed (1993) discussed the significance of the simultaneous solution of mass, energy and leakage equations in design and selection of laboratory control and operating variables. That paper also demonstrated the effect of air density changes on the variables. A laboratory space simulation was used to investigate the influence of heat load on selection of laboratory design parameters and the dynamics of laboratory thermal environment (Ahmed et al. 1996). The current paper extends the study to include the laboratory HVAC and control systems.

Figure 1 shows a schematic of a laboratory HVAC system showing the major physical variables. Laboratory pressure and temperature, P and T are the internal environmental variables which need to be maintained within the specified limits. The conditioned supply air is sent to the laboratory at a pressure P_S, temperature T_S and at a volumetric flow rate of $\dot{v}_s$. The heating coil entering and leaving water temperatures are $T_{f,i}$ and $T_{f,o}$ while the water flow rate through the coil is $\dot{v}_f$. The total fume hood exhaust volumetric flow rate, $\dot{v}_{fh}$, leaves at the room pressure and temperature. There is also a general exhaust of $\dot{v}_{ex}$ at room pressure and temperature. Infiltration $\dot{v}_{ad}$ from adjacent spaces at P_{ad} and T_{ad} occurs.

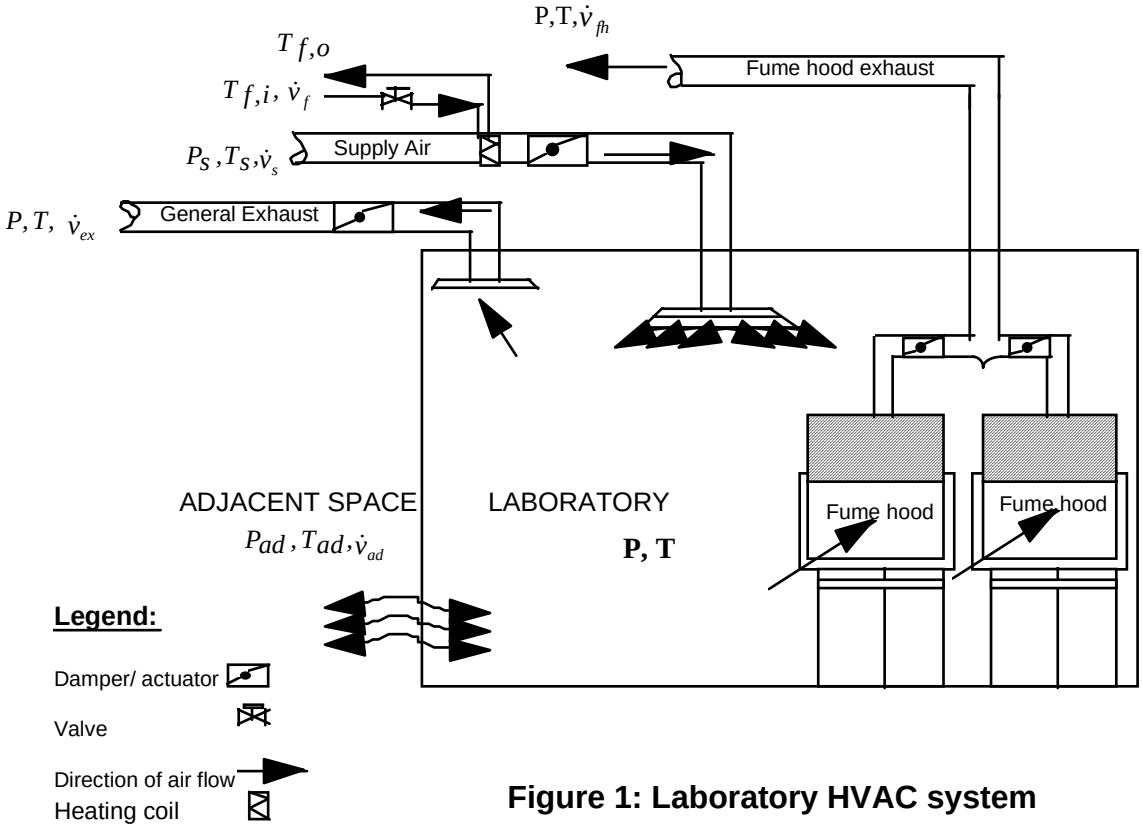

Figure 1: Laboratory HVAC system

Providing safety and comfort are the two basic functions of a laboratory HVAC system. Effluents are exhausted through the fume hood exhaust and leakage from the laboratory. The fume hood is controlled to maintain a constant average face velocity of entering room air. The laboratory pressure (P) is maintained lower than the adjacent space pressure (P_{ad}) to ensure that air does not leak out of the laboratory. However, in certain laboratories such as clean rooms the interior pressure is kept higher than the adjacent space ($P>P_{ad}$) to prevent the flow of any foreign particles from the adjacent space. The control system is responsible for maintaining the values of selected process variables, laboratory temperature T and pressure differential, P_{ad}-P (denoted as ΔP), within specified ranges. In addition, the control system measures and controls other control variables such as the volumetric flow rates of supply air, $\dot{v}_s$, general exhaust, $\dot{v}_{ex}$ and coil water, $\dot{v}_f$.

The objective of this paper is to present a dynamic simulator developed for use in the control strategies for a laboratory HVAC system. The simulator is based on physical mechanisms and includes the laboratory envelope, air flow system, heating and cooling coils, and a proportional-integral controller. Many of the components of the simulator have been validated through experiment (Ahmed 1996). The transient response of the controlled variables for given forcing functions are generated by the simulator. A proportional-integral controller is then combined with a model-based predictor to provide control. The controller is shown to provide the rapid control action needed to meet comfort and safety criteria for typical conditions that occur in laboratories.

SIMULATION MODEL:

The simulation model consists of the laboratory space, heating coils, air and water flow and a controller. The models for each of these components is described in the following sections.

*Laboratory space***:**

The purpose of the laboratory space model is to simulate the response of environmental parameters, temperature and pressure, when subjected to the forcing functions commonly found in a real laboratory. The space model assumes that the air is an ideal gas, the effect of humidity on properties is negligible, laboratory air temperature and pressure are spatially uniform at any instant of time, adjacent space temperatures and pressures and supply duct pressure are constant, internal heat generation is purely sensible, and heat conduction is one dimensional through the walls.

The conservation of mass of air in the laboratory is given by

$$\frac{dm}{dt} = \dot{m}_s + \dot{m}_{ad} - \dot{m}_e \tag{1}$$

Because of the change in pressure and temperature in the laboratory, the mass of the air in the laboratory is not constant. The mass flow is related to the volumetric flow rate and density by

$$\dot{m} = \dot{v}\rho \tag{2}$$

Using the ideal gas law for the density,

$$\rho = \frac{P}{RT} \tag{3}$$

the mass flow can be written in terms of pressure, temperature, and volume flow rate as

$$\dot{m} = \frac{P\dot{v}}{RT} \tag{4}$$

The above expression shows the dependence of mass flow rate on both pressure and temperature. The density of air ρ is usually treated as a constant in HVAC system studies, but it is important to include the variation in density with temperature and pressure in the laboratory simulator. Using equations 3 and 4, equation 1 becomes

$$\frac{d(PV/RT)}{dt} = \frac{P_s\dot{v}_s}{RT_s} + \frac{P_{ad}\dot{v}_{ad}}{RT_{ad}} - \frac{P\dot{v}_e}{RT} \tag{5}$$

Differentiating the first term by parts and canceling the gas constant, R, on both sides results in

$$\frac{V}{R}\left[\frac{1}{T}\frac{dP}{dt} - \frac{P}{T^2}\frac{dT}{dt}\right] = \frac{P_s\dot{v}_s}{RT_s} + \frac{P_{ad}\dot{v}_{ad}}{RT_{ad}} - \frac{P\dot{v}_e}{RT} \tag{6}$$

The conservation of energy equation includes the energy carried in and out by flows and heat flows.

$$\frac{dU}{dt} = \sum h_i\dot{m}_i - h_e\dot{m}_e + \dot{q}_{gen} + \dot{q}_{tr} \tag{7}$$

where *i* denotes all inflow, *e* denotes all outflow, $\dot{q}_{tr}$ is the internal energy generation and $\dot{q}_{tr}$ is the heat transfer through the envelope.

The Equation 7 can be further expanded in terms of mass and specific internal energy as

$$m\frac{du}{dt} + u\frac{dm}{dt} = \sum h_i\dot{m}_i - h_e\dot{m}_e + \dot{q}_{gen} + \dot{q}_{tr} \tag{8}$$

Taking derivatives of left hand side of equation 8, assuming a constant room volume V, and introducing the ideal gas equation for internal energy u= $c_V T$, the following equation is obtained.

$$\frac{PV}{RT} c_v \frac{dT}{dt} + \frac{Tc_v V}{RT} \frac{dP}{dt} - c_v T \frac{PV}{RT^2} \frac{dT}{dt} = \sum h_i \dot{m}_i - h_e \dot{m}_e + \dot{q}_{gen} + \dot{q}_{tr} \quad (9)$$

Canceling the first and third terms on the left hand side, introducing inflows and outflows in terms of volumetric rates, and expressing the enthalpy of air as $dh = c_p dT$,

$$c_v \frac{V}{R} \frac{dP}{dt} = \frac{P_s \dot{v}_s}{RT_s} c_p T_s + \frac{P_{ad} \dot{v}_{ad}}{RT_{ad}} c_p T_{ad} - \frac{P \dot{v}_e}{RT} c_p T + \dot{q}_{gen} + \dot{q}_{tr} \quad (10)$$

Equation 10 can be simplified to,

$$c_v \frac{V}{R} \frac{dP}{dt} = \frac{P_s \dot{v}_s}{R} c_p + \frac{P_{ad} \dot{v}_{ad}}{R} c_p - \frac{P \dot{v}_e}{R} c_p + \dot{q}_{gen} + \dot{q}_{tr} \quad (11)$$

Equations 6 and 11 are the governing equations for the laboratory and solving them simultaneously will yield the room pressure and temperature response to given forcing functions. In Equations 7 to 11, the term $\dot{q}_{tr}$ represents heat transfer through the room envelope. The mode of heat transfer through room envelope is assumed to be pure conduction with surface convection to room air. The envelope usually consists of four walls, a ceiling and a floor. The rate of heat transfer from surface to room air is calculated using simple convection relations. This is a valid assumption since the laboratory spaces are usually interior zones and not exposed to outdoor conditions.

$$\dot{q}_{tr} = \sum hc_u A_u (T_u - T) \quad (12)$$

where, subscript u represents the u th component of room envelope. More explicitly, the above equation can be written as

$$\dot{q}_{tr} = \sum_{j=1,4} hc_{r,w} A_{r,w} (T - T_{w,j}) + hc_{r,fl} A_{r,fl} (T - T_{fl}) + hc_{r,cl} A_{r,cl} (T - T_{cl}) \quad (13)$$

Envelope models:

The transient conduction through the room envelope from the surrounding environment can be treated in different ways depending on the construction of the walls. Interior panel walls are commonly constructed of metal sheets separated by air or insulation. In this situation a lumped capacitance approach (Incropera and DeWitt 1985) is appropriate. For exterior walls made of concrete and similar materials, a finite difference approach is appropriate (Incropera and DeWitt, 1985). These different approaches have been evaluated for laboratory systems (Ahmed 1996).

In order to generate a general purpose simulator applicable to all laboratories, a single equivalent wall model was used. In this approach, the walls are treated as having an equivalent capacitance and are coupled to the laboratory environment through an equivalent conductance as shown in Figure 2. The values of the capacitance and conductance may be determined from a combination of fundamental heat transfer relations (ASHRAE 1993) and calibration experiments (Ahmed, 1996).

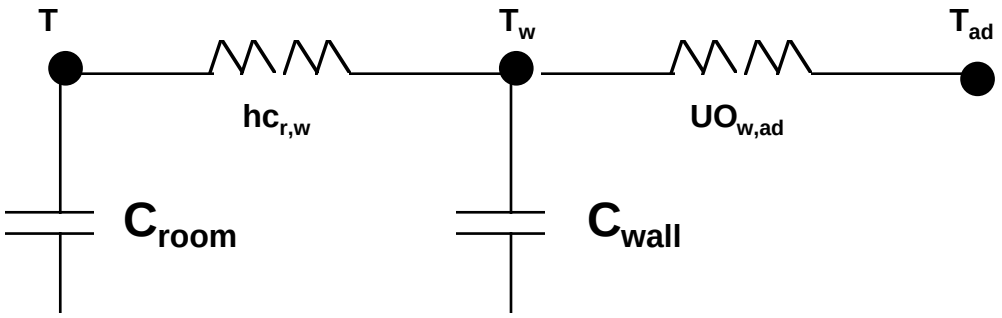

Figure 2: Thermal network for single equivalent wall

Infiltration:

The pressure differential between a laboratory and surrounding spaces causes infiltration. The infiltration through envelope holes and cracks is adequately expressed by an equation of the type shown (Eqn. 14) which has been found to be adequate in previous studies (Shah 1980; ASHRAE 1989).

$$\dot{v}_{ad} = K_l(\Delta P)^n \qquad (14)$$

The infiltration equation couples the volumetric flow rate of infiltrating air and differential pressure across the envelope. Equation 14 is coupled to equations 6 and 11 through $\dot{v}_{ad}$ and P_{ad}. The parameters used in the envelope and infiltration models are given in Table 1.

Heating coil:

A heating coil model for the simulator is needed that is simple and yet which will provide reasonable accuracy in simulating coil characteristics. The effectiveness model (Braun et al. 1987) was used. The schematic of a coil along with the effectiveness plot is shown in Figure 3.

The heating coil model assumes negligible heat loss from the heat exchanger to the surroundings, constant fluid properties and negligible fouling factors. The basic coil heat transfer equation is the heat flow to the air:

$$\dot{q} = C_a(T_{a,o} - T_{a,i}) \qquad (15)$$

The coil effectiveness ε is defined as the ratio of actual to maximum heat transfer rate or

$$\varepsilon = \frac{\dot{q}}{\dot{q}_{\max}} \qquad (16)$$

The maximum rate of heat transfer occurs when the fluid with the minimum product of flow rate and specific heat leaves at the entering temperature of the other fluid. Hence, actual coil heat transfer rate, $\dot{q}$ can be rewritten as

$$\dot{q} = \varepsilon\, C_{\min}(T_{f,i} - T_{a,i}) \qquad (17)$$

Combining equations 15, 16 and 17 yields the outlet air temperature

$$T_{a,o} = T_{a,i} + \varepsilon\left(\frac{C_{min}}{C_a}\right)(T_{f,i} - T_{a,i}) \qquad (18)$$

The heating coil effectiveness was calculated assuming a cross flow heat exchanger (Incropera & Dewitt 1985)

$$\varepsilon = 1 - e^{\left(-\frac{1}{C_r}\left(1 - e^{-(C_r NTU)}\right)\right)} \quad (19)$$

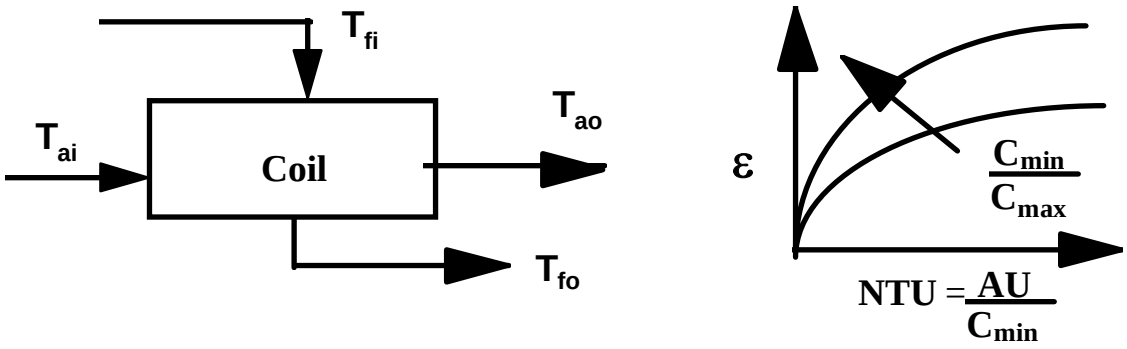

Figure 3: Coil schematics and effectiveness plot

Where,

$C_r = \frac{C_{\min}}{C_{\max}}$, $NTU = \frac{hc_{coil} A_{coil}}{C_{min}}$, $C_{min} = min(C_f, C_a)$

and $C_{max} = max(C_f, C_a)$

The coil number of transfer units, NTU is estimated based on design values of C_{min} and ε. Published coil data are used to develop a functional relationship between coil NTU, ε and the ratio of C_{min} and C_{max} (Kays and London 1964). Once the coil NTU is determined, it may be assumed constant with flow rate. However, coil effectiveness ε will change with the variation in coil capacitance C_{min} and C_{max}. The use of these design parameters is a simple yet effective way of selecting coil parameters. The coil simulation parameters are listed in Table 3.

The coil dynamic response is represented assuming a first order system (U.S. Dept. of Commerce 1984; Pearson 1974) as follows:

$$\tau_{coil} \frac{dT_{ao}}{dt} + T_{ao} = T_{ao,sp|\,(t-t_o)} \quad (20)$$

The above equation indicates that $T_{a,o}$ will approach the setpoint exponentially. The rate with which the outlet temperature approaches the setpoint is determined by the coil time constant, τ_{coil}.

*Damper/ Valve***:**

Variable fluid resistance devices such as dampers and valves exhibit the same fluid characteristics and the performance can be expressed in terms of identical variables. The valves and dampers are represented by the models as used in the HVACSIM$^+$ simulation program (U.S. Dept. of Commerce 1984). For clarity, only the term damper will be used although the model is also valid for valves.

The air flow model consist of a duct section, a damper, and a duct section downstream of the damper shown schematically in Figure 4.

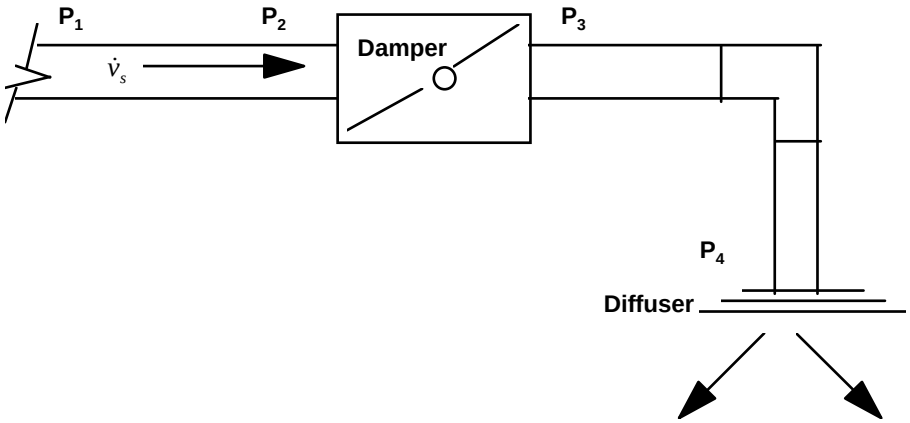

Figure 4: Damper schematics

The model computes the flow rate given the damper position and upstream and downstream pressures. The damper position is linked to the actuator position which is commanded by the controller. The model assumes that the flow is fully developed, density changes are negligible, heat transfer from duct walls is neglected, and the frictional coefficient in the flow range under consideration remains constant. The pressure difference is assumed to be proportional to the square of the flow rate.

$$P_1 - P_2 = K_{12}(\dot{v}_s)^2 \tag{21}$$

$$P_2 - P_3 = K_{23}(\dot{v}_s)^2 \tag{22}$$

$$P_3 - P_4 = K_{34}(\dot{v}_s)^2 \tag{23}$$

The coefficients K_{12} and K_{34} are evaluated based on design conditions and standard HVAC design procedures. K_{23} is expressed as (U.S. Dept. of Commerce 1984),

$$\mathrm{K}_{23} = \frac{W_f K_o}{[(1-\lambda)r + \lambda]^{2.0}} + (1 - W_f)K_o\mu^{(2r-2)} \tag{24}$$

In equation 24, the parameter W_f determines the non-linearity of the damper. A value of W_f of 0 indicates a linear damper whereas 1.0 means an exponential damper. The term λ indicates a leakage constant since most dampers leak. The damper flow resistance coefficient at fully open position is K_o and r represents the normalized (0 -1) position commanded by the controller. The term μ is a damper parameter and its value was set equal to the leakage parameter λ in simulation.

The flow through the damper can be also predicted by representing the installed characteristics with the authority, a. The installed authority dictates the ultimate performance of a damper in a system. For example, an inherently linear damper will exhibit non-linear performance as the authority becomes smaller. Therefore, by using system authority as a simulation variable it is possible to duplicate the installed performance of a damper. The system authority can be defined as the ratio between the pressure drop across the damper and the total pressure drop when the damper is fully open. Mathematically,

$$\boldsymbol{a} = \frac{(P_2 - P_3)|_{dfo}}{(P_1 - P_4)|_{dfo}} \qquad (25)$$

For a specified authority, the value of K_{12} can be determined from equations 21 to 25 and the flow rate.

The values of K_{12} for various authority are listed in Table 2 for a specific linear damper. The simulated characteristics of a linear damper are shown in Figure 5 for different values of authority. The plot shows that a linear damper exhibits non linear characteristics as the authority decreases. The representation used in the damper model is employed in the valve model.

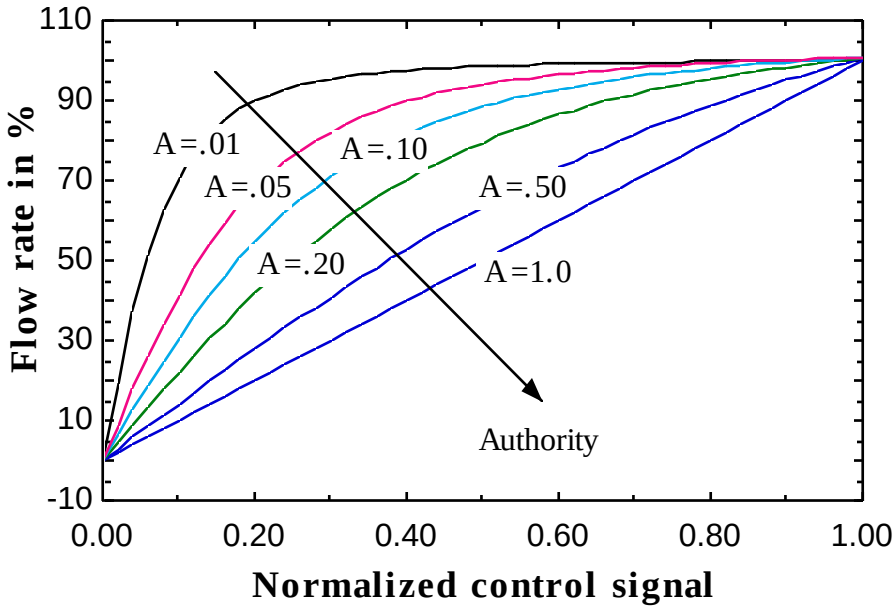

Figure 5: Characteristics of a linear damper

Actuator:

A simple first order linear model with a dead time was assumed for the pneumatic actuator (U.S. Dept. of Commerce 1984). The dead time implies that at any instant t, the normalized position of the actuator, r_{ac}, is affected by the value of commanded position, r_{sp}, at t_o units of time earlier. The relation is

$$\tau_{act} \frac{dr_{ac}}{dt} + r_{ac} = r_{sp|_{(t-t_o)}} \qquad (26)$$

By choosing different actuator time constants τ_{act} and dead times t_o it is possible to simulate different actuator response profiles. Equation 26 is valid for a pneumatic actuator such as widely used in the laboratory control system to produce a fast response. It also provides the added benefit of safety since it opens fully at a failure mode.

Room temperature sensor:

The room air temperature is usually sensed using a temperature sensor installed on the wall that does not provide a direct measure of the actual room air temperature. A simple lumped capacitance model used as follows to relate the sensor value to the room and wall temperature.

$$\frac{dT_{st}}{dt} = C1_{st}(T_{pw} - T_{st}) - C2_{st}(T_{st} - T) \quad (27)$$

The coefficient $C1_{st}$ is the ratio of conduction heat transfer coefficient between the wall and temperature sensor and sensor thermal capacitance. $C2_{st}$ is the ratio of the convection coefficient to thermal capacitance. The coefficients were determined using measured values of sensor output. Based on experimental results (Ahmed 1996) a $C1_{st}$ of 0.10 (minutes^{-1}) and $C2_{st}$ of 0.12 (minutes^{-1}), were selected for simulation.

Feedback controller:

The feedback controller uses the error between the setpoint and the measured variable as input. The most common approach of employing feedback is the traditional linear Proportional- Integral-Derivative (PID) algorithm. In a PID controller, the tuning parameters are derived for a specific operating range. Feedback control is simple to implement and performs well as long as the operating range and the setpoints do not vary significantly. In most HVAC applications, however, derivative control adds unneeded complexity and tuning difficulty (Haines and Hittle 1983). A well tuned PI can achieve the desired response without the needed derivative control action. The PI controller selected (Bekker et al. 1991) was developed for common HVAC processes such as coils and valve/ damper actuators, which are often modeled as first order linear systems with delay. These models are also used in the simulator to represent coil and actuator dynamics as a part of the laboratory simulator.

The form of the PI controller in digital representation (Mollenkamp 1981) can be expressed as follows:

$$C_{s,m} = C_{s,m-1} + P_g(e_m - e_{m-1}) + I_g S_t e_m \quad (28)$$

where,

$C_{s,m}$ is controller output at the mth sample time, $C_{s,m-1}$ is the controller at the m-1th sample time, e_m is the error between the actual value and the setpoint of a process variable at the mth sample time, and e_{m-1} is the error between the actual value and the setpoint of a process variable at the mth sample time. The PI controller described by equation 28 is easy to use in digital controllers that are commonly used in building automation systems. The selected form of PI controller is also easy to initialize in a digital controller. Caution is needed with the PID digital controller to avoid the runway of the integral term known as “Integral Windup”. To solve such problem in the simulation, the value of the integral term was limited to 30% of the maximum normalized control signal of 1.0.

The gains P_g and I_g are tuned as per the following equations.

$$I_g = \frac{1}{d_t S_g} e^{-1} \quad (29)$$

and

$$P_g = \frac{\tau}{d_t S_g} e^{-1} \qquad (30)$$

Where, d_t is delay time and S_g is system gain. The tuning of the PI controller is based on the method proposed by Bekker et al. (1991). The PI gains for various control loops are shown in Table 4.

SIMULATION RESULTS:

The simulation was carried out using Engineering Equation Solver(EES) software (Klein and Alvarado 1997). The EES uses a variant of Newton's method to solve non-linear algebraic equations while a variant of the trapezoid rule with a second order predictor- corrector algorithm is used for solving differential equations. Although the laboratory simulator is applicable to any laboratory HVAC system, a Variable air Volume (VAV) system is considered here. The VAV laboratory system is growing in popularity in the laboratory industry due to its ability to reduce energy use. However, a VAV system poses new challenges to the control system to maintain both space comfort and safety criteria. Sudden changes in the laboratory operating conditions as a result of fume hood operation or generation of internal load need to be accommodated. Several control sequences were selected to test the simulator using a simple PI controller to control over the entire domain of normal operation in a VAV laboratory system (ASHRAE 1995, Neuman and Guven 1988; Marsh 1988). The pressure sequence is directly coupled to the safety requirements while the temperature sequences are relevant to the comfort constraints.

Pressure control:

The room pressure is typically controlled in terms of a differential instead of an absolute value. The differential is defined as a difference between a reference space (i.e. an adjacent corridor) and the laboratory space. The differential pressure is typically positive within a range of .00125 to .0125 kPa (.005 to .05 inches of water). The essence of a pressure control sequence is to modulate the supply flow in order to maintain the room differential pressure in response to a step change in the fume hood exhaust. Two different disturbance sequences, as shown in Figure 6, were considered for the simulations. First, the total laboratory fume hood exhaust flow is reduced from a maximum of 1132.8 L/s (2400 cfm) to 236 L/s (500 cfm) and then increased to 1132.8 L/s again. The corresponding supply flow rates needed to maintain a space temperature of 21.11 ^{o}C (70 ^{o}F) and Δp of .0125 kPa are 1065 L/s (2257 cfm) and 168.5 L/s (357 cfm). The thermal effect is decoupled from the pressure effect by assuming that the temperatures of supply, exhaust and infiltration air are constant at 21.11 ^{o}C (70 ^{o}F).

The simulation sample time is chosen to be 0.1 seconds which is representative of the current state-of-the-art HVAC process controllers. Dorf (1980) recommended a minimum of 2-3 samples per process time constant for a digital controller. Hence, the simulation sample time of 0.1 is adequate compared to the time constant of 0.3 seconds of the fast acting damper actuator considered in simulation. The time constant of 0.3 seconds was chosen in order to achieve a pneumatic damper stroke time of 2 seconds which is necessary for a lab control system (Ahmed 1996). The simulation sample time of 0.1 second means that about 17-18 samples are obtained during damper stroke time of about 2 seconds, which is also adequate (Haines and Hittle 1983).

The steady state mass balance and infiltration equations are used to solve for the supply flow setpoint. The steady state mass balance (equation 6) written in terms of setpoints is

$$\frac{P_{s,sp}\dot{v}_{s,sp}}{T_{s,sp}} + \frac{P_{ad,sp}\dot{v}_{ad,sp}}{T_{ad,sp}} - \frac{P_{sp}\dot{v}_{e,sp}}{T_{sp}} = 0 \quad (31)$$

The infiltration relation (from equation 21) is

$$\dot{v}_{ad,sp} = K_l(\Delta P_{sp})^n \quad (32)$$

The laboratory pressure differential, ΔP_{sp}, is defined as a differential as follows:

$$\Delta p_{sp} = P_{ref,sp} - P_{sp} \quad (33)$$

In above equations laboratory supply air flow rate setpoint, $\dot{v}_{s,sp}$; total laboratory exhaust setpoint, $\dot{v}_{e,sp}$; and supply air discharge temperature setpoint, $T_{s,sp}$ are unknowns with others unknown from the design data. The total laboratory exhaust is a sum of general exhaust and exhaust from fume hoods, and given by:

$$\dot{v}_{e,sp} = \dot{v}_{fh,sp} + \dot{v}_{ex,sp} \quad (34)$$

In a VAV laboratory, the fume hood exhaust setpoint is a known quantity for each position of the fume hood sash. Hence, by determining the setpoint for total laboratory exhaust, the general exhaust setpoint will be known. For the pressure control sequence, $\dot{v}_{ex,sp}$ is zero since the general exhaust damper is only opened during cooling sequence as explained in the next sequences. The method of calculating laboratory supply air flow rate setpoint, $\dot{v}_{s,sp}$, depends on the selection of pressure control strategy.

There are two common methods of laboratory space pressure control. In the first approach, the supply flow setpoint is determined by assuming a fixed difference between the laboratory exhaust and supply flow setpoint. This method is known as flow tracking. In a direct approach a differential pressure sensor, is usually mounted near the entrance door. The error between the differential pressure setpoint and the actual value is calculated first and then fed into a PID algorithm which produces an output of supply flow setpoint. There are two severe limitations of the direct approach; exceptional sensitivity to very small values of pressure differential (i.e. .0025 kPa), and the measured pressure differential becomes zero when the door is opened Hitchings (1994). The flow tracking method is more prevalent in the industry.

The method of calculating the supply flow setpoint in flow tracking has serious limitations as often the difference in flow is assumed based on experience as illustrated in the published literature (Ahmed 1993; Ahmed et al. 1993). The space may suffer from over- or under-pressurization if the difference in flow is selected incorrectly. The PI control strategy models, as used in the simulations, are shown in Figure 6.

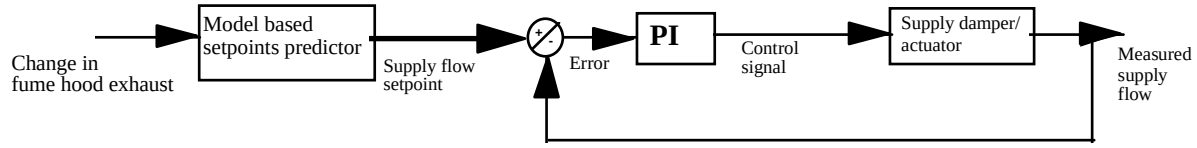

Figure 6: Schematic of PI for pressure control sequence

Figure 7 shows the simulated result for a pressure control sequence assuming a linear damper (i.e. a=1.0 in Figure 4). The assumption of linear damper is reasonable since the primary objective in this paper is to demonstrate the feasibility of the laboratory simulator. In fact, both linear and non-linear damper characteristics with different authorities were considered in detailed analysis of the laboratory simulation model (Ahmed 1996). The PI controller also tuned for the linear damper

characteristics. This is appropriate since HVAC control equipment manufacturers usually assume that the valves, dampers and actuators are linear in calibration. Further, during the commissioning process these devices are usually tuned at fully open positions. As a result the pressure drop across the control equipment is maximum and the authority is close to unity.

The fume exhaust flow in Figure 7 suddenly decreases at the start of the sequence. The differential pressure ($\Delta P = P_{ad} - P$) momentarily becomes negative meaning that the room remains at a higher pressure than the adjacent room until the supply flow reduces to match the exhaust flow for the correct differential. The reverse takes place when the fume hood exhaust is increased from a minimum flow. The PI controller has zero offset under steady state.

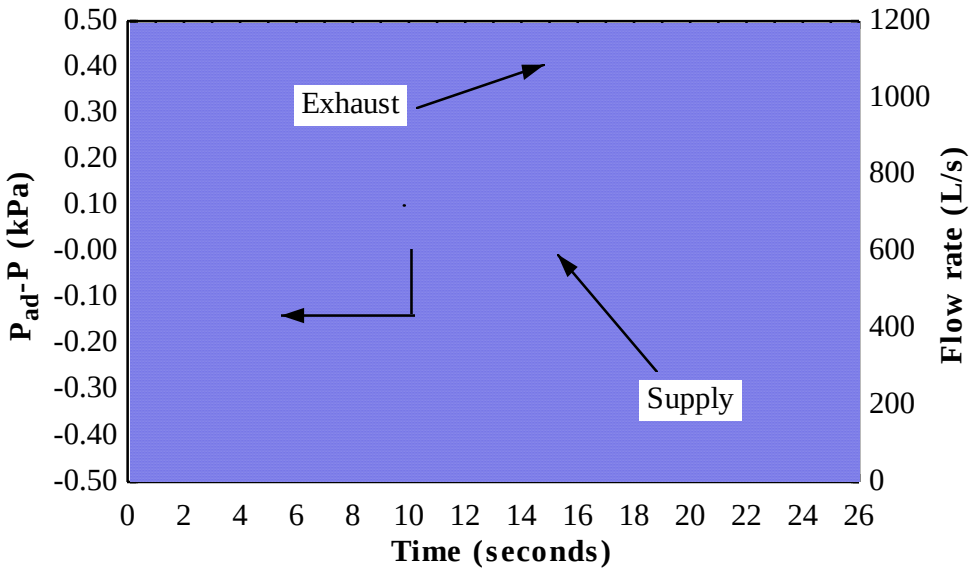

Figure 7: Disturbance in laboratory exhaust flow for pressure control

Temperature control during cooling:
Activities in a laboratory such as autoclaves, ovens and occupancy generate heat and are the primary disturbing forces that activate this sequence. When the internal generation suddenly increases, the room temperature rises. The only cooling source available is the supply air stream at 12.78 ^{O}C. (55 ^{O}F). But, the supply flow cannot be increased unless the exhaust flow is also increased in order to maintain the differential pressure constraint. However, the laboratory exhaust flow cannot be increased unless the fume hoods are opened manually. To allow more supply air the general exhaust needs to be opened.

For the temperature control loops, the simulation sample time is selected to be 10 seconds. This is much longer than 0.1 seconds considered for the pressure control loops. The pressure response is much faster than the thermal response and the pressure transients are essentially over before the thermal response is significant. This was noted during the analysis of simulated results obtained by considering simultaneous pressure and thermal responses (Ahmed 1996). Accordingly, the transient energy and mass balance equations (i.e. Equations 6 and 11) are rewritten assuming that the pressure is constant as

$$V\left[-\frac{P}{T^2}\frac{dT}{dt}\right]=\frac{P_s\dot{v}_s}{RT_s}+\frac{P_{ad}\dot{v}_{ad}}{RT_{ad}}-\frac{P\dot{v}_e}{RT} \quad (35)$$

$$\frac{P_s\dot{v}_s}{R}c_p+\frac{P_{ad}\dot{v}_{ad}}{R}c_p-\frac{P\dot{v}_e}{R}c_p+\dot{q}_{gen}+\dot{q}_{tr}=0 \quad (36)$$

The assumption that the pressure is constant is justified from a practical sense since in reality the fast flow loops will always achieve the setpoint before the next room temperature is sampled. The schematic of PI control for flow is shown in Figure 8.

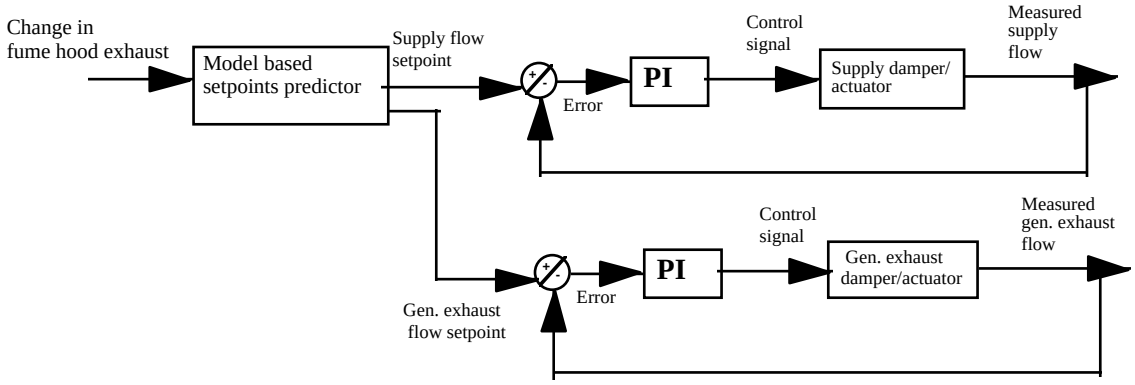

Figure 8: Schematics of PI for Temperature control- cooling sequence

In the cooling sequence, both supply and general exhaust flow setpoints need to be determined. A common approach in a feedback controller is to use another PID algorithm which acts upon the error between the room temperature setpoint and the actual value. The PID output is the general exhaust flow setpoint. The supply flow setpoint is then calculated assuming a fixed differential with respect to the general exhaust flow setpoint. Addition of another PID loop further complicates the tuning process. In Figure 8, if a PID loop is used instead of a model based predictor, a total of 7 tuning parameters need to be evaluated for the two PI and the one PID coupled loops. The performance of coupled loops also suffers when the operating condition shifts from the tuned condition, a common feature of a laboratory control system. On the other hand, a model based setpoint predictor will require less tuning and performance will not be dependent on the operating conditions.

The flow setpoints of general exhaust and consequently of supply are determined using steady state energy, mass and infiltration equations as discussed in the pressure control sequence. However, the energy equation now contains a room thermal load (sum of terms $\dot{q}_{gen}$ and $\dot{q}_{tr}$ in equation 36). The predicted load is calculated based on the room air temperature and the supply flow rate at the preceding time step t-1 as shown in equation 37.

$$\dot{q}_{load|ss}=\dot{v}_{e,(t-1)}\rho c_p T_{(t-1)}-\dot{v}_{s,(t-1)}\rho c_p T_s-\dot{v}_{ad,sp}\rho c_p T_{ad} \quad (37)$$

In the tuning process the general exhaust damper flow loop was tuned first and then the supply flow loop. Linear dampers were assumed for both general and exhaust flows. Figures 9 and 10 illustrate the temperature response for decreasing and increasing internal loads respectively. The internal load was increased five fold from its initial value of 87.0 kJ/min. (82.50 Btu/min.) to 435 kJ/min (412.50 Btu/min.), while in the second case, the internal load is decreased by the same proportion. The total load includes the internal generation and the heat transfer from the wall elements, ceiling and the floor. The figures show both the input and predicted loads; the load

predicted by equation 37 agrees extremely well with the input load. A good load prediction is a precondition of achieving good control. In both cases, The PI controller performed very well in terms of setpoint tracking accuracy and response time and PI control loop quickly settles to the desired setpoint of 21.11 ^{o}C (70 ^{o}F).

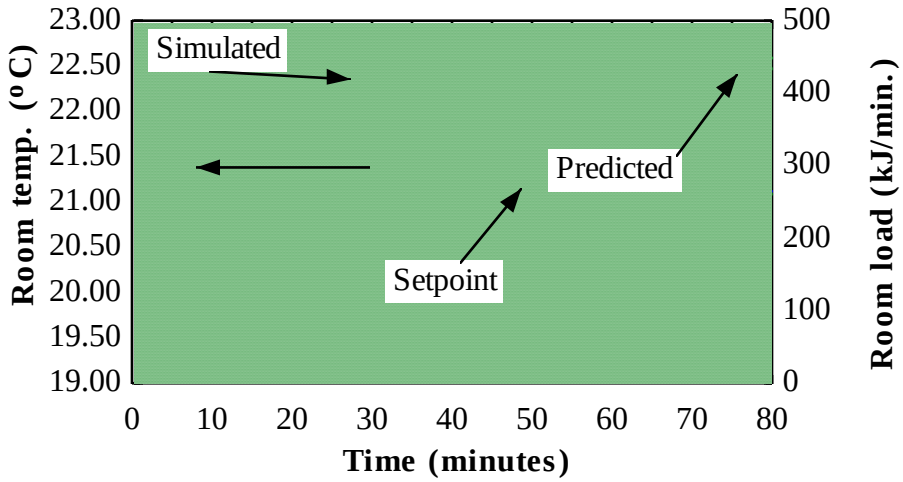

Figure 9: Performance of temp control- cooling due to increase in cooling load

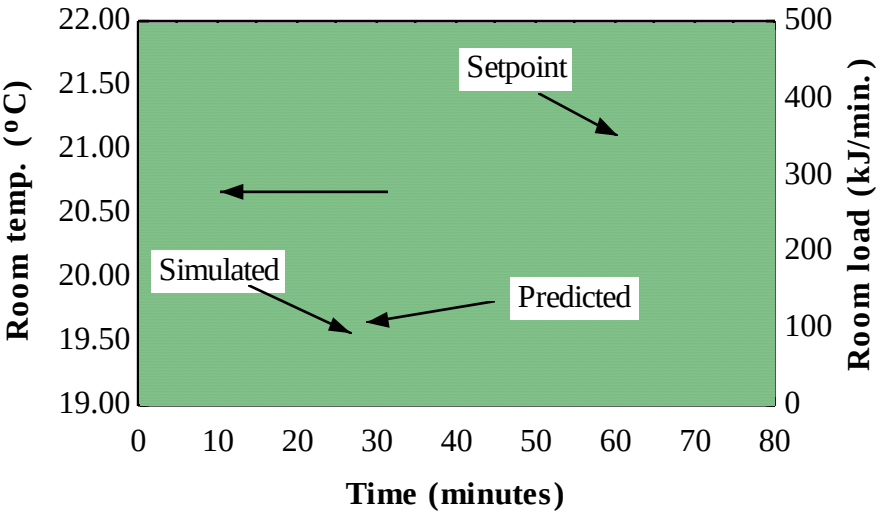

Figure 10: Performance of temp control- cooling due to decrease in cooling load

*Temperature control during heating**:***

In most VAV applications, the supply air is discharged into the laboratory space at 12.78 ^{o}C (55 ^{o}F). However, when the laboratory exhaust suddenly increases due to the fume hood sash opening, the supply flow rate also increases accordingly. The new supply flow rate at a constant 12.78 ^{o}C may exceed the requirement of the normal cooling demand and the room temperature may drop below the setpoint. The local reheat valve needs to open to increase the supply air temperature and maintain the room temperature setpoint.

Two separate disturbance sequences are considered for heating. In the first sequence, the disturbance is caused by a sudden increase in the fume hood exhaust (212 to 1156 L/s or 450 to 2450 cfm) due to the sash opening from minimum to full position at time t=20 seconds. The internal thermal load remains constant. The supply flow rate and temperature setpoints are determined using the same set of steady state equations, as described in the cooling control sequence. The control strategy is shown in Figure 11.

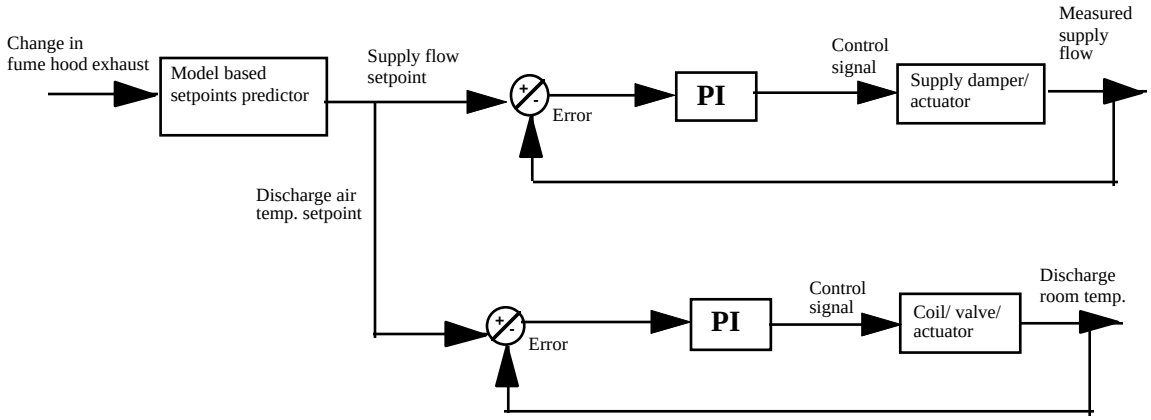

Figure 11: PI controller for temperature control- heating due to ventilation

The second control sequence considered for heating is a simultaneous change in the space internal load and exhaust flow. The laboratory initially has a maximum laboratory exhaust flow (1156 L/s) and supply flow that maintain the room temperature and differential pressure constraints. Then at time t=20 sec., the total laboratory exhaust is decreased (620 L/s or 1313 cfm) and at the same time the internal load (174 kJ/min. or 165 Btu/min.) is generated. As a result, the space needs partial heating. Figure 12 shows the schematics of a PI controller for heating with the room load

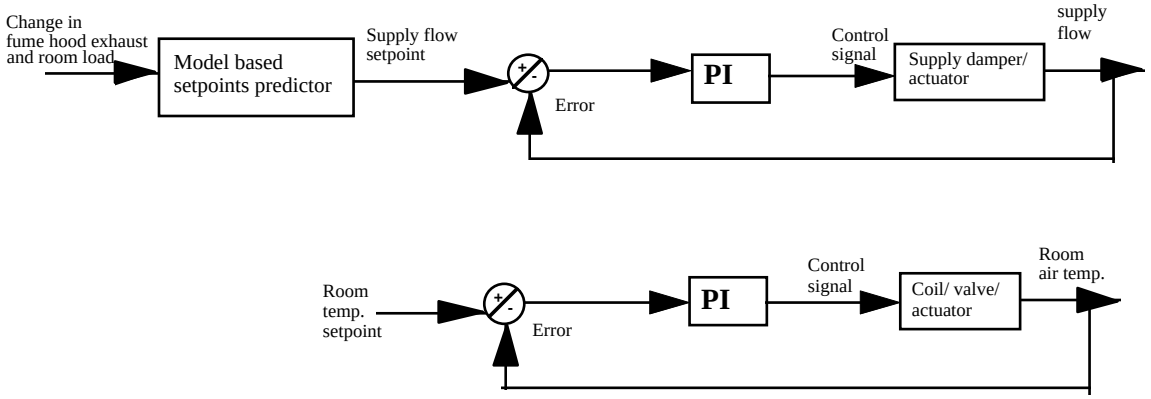

Figure 12: PI controller for temperature control- heating with room load.

The control strategy is very similar to the previous sequence without the room load. However, the model based predictor now includes the predicted load in order to determine supply flow and temperature setpoints. The room temperature setpoint is used in the feedback block. As with the control during cooling, the laboratory pressure is assumed constant.

For the heating sequence, the sample time is chosen to be 2 seconds. The tuning of the valves for the PI are done in the same way as described before with the pressure control sequence. Identical linear characteristics are chosen for the damper and valve for two heating sequences discussed

above. Figure 13 shows the performance of controller in terms of room and discharge air temperatures for heating sequence due to ventilation.

The initial undershoot in room temperature is expected as the sudden increase in room total exhaust causes the supply flow at 12.78 ^{o}C (55 ^{o}F) to increase. The increased supply flow rate is in excess of the required amount to offset the room thermal load. The room temperature falls before the coil water valve is opened in order to provide heating and offset the sudden increase in room ventilation load. The initial undershoot in room temperature is less than 0.278 ^{o}C (0.50 ^{o}F) for PI controller.

The PI controller performance for heating with the room load is shown in Figure 14. As the sudden load is imposed, the room temperature increases before the prediction model can determine that less heating is needed and signal the control system to close the valve. The discharge air temperature then settles to a new steady state value.

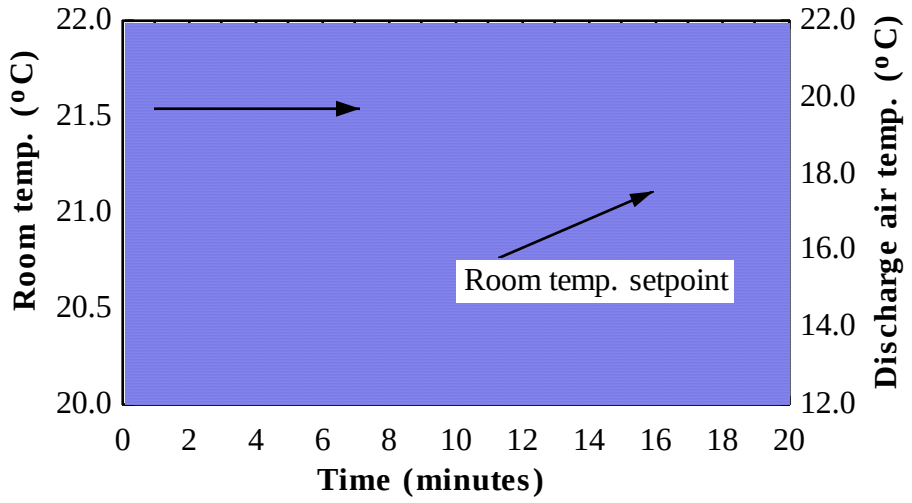

Figure 13: Temp. response for heating due to ventilation

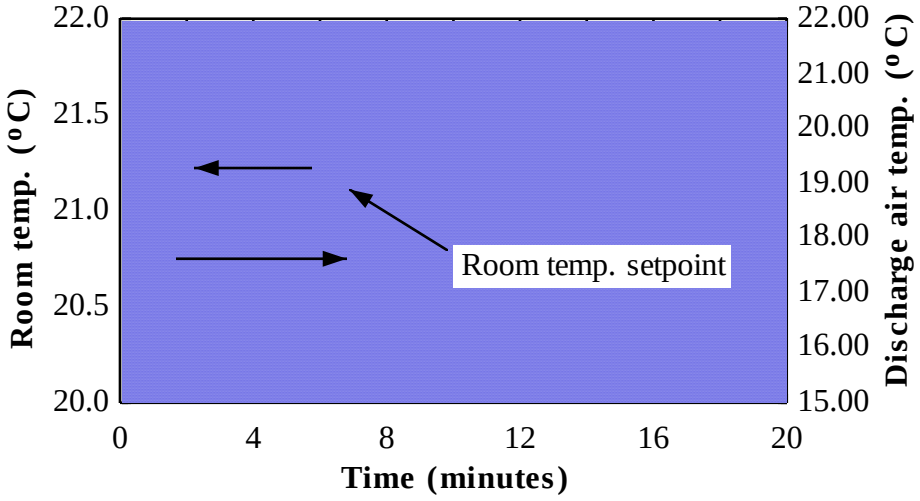

.

Figure 14: Temp. response for heating with room load

CONCLUSIONS:

The conclusions that can be drawn from this paper are summarized as follows:

- The laboratory environment is unique in terms of the comfort and safety requirements and the operation dynamics. This paper presents a laboratory simulation model that contains the components most commonly found in a laboratory environment. The simulator is suitable for evaluating the dynamic response of a laboratory and HVAC control systems.

- The feasibility of the simulation model has been demonstrated by simulating a controller that combines PI and model based predictor for three most common control sequences unique to the VAV laboratory. The controller has been found capable of maintaining the laboratory pressure and temperature within desirable limits.

- The simulator can be used as a design tool to find the interactions between the operating variables and the transient and steady state behavior of the lab environment. Use of simulation in the design phase will provide better laboratory operation and enhance comfort and safety.

REFERENCES:

Ahmed, O., "Model based control of laboratory HVAC systems," *Ph.D. thesis,* University of Wisconsin- Madison, WI., 1996

Ahmed, O., J.W. Mitchell., and S.A. Klein., "Influence of heat load on selection of laboratory design parameters and dynamic performance of laboratory environment," *ASHRAE Transaction*, V.102, Pt.1, 1996

Ahmed, O., "A Design Method for Laboratory Pressurization," *CLIMA 2000 conference*, London, U.K., 1993a

Ahmed, O., J.W. Mitchell., and S.A. Klein., "Dynamics of Laboratory Pressurization," *ASHRAE Transaction*, 1993b

American Society of Heating, Refrigerating and Air Conditioning Engineers., "1989 Fundamentals Handbook," ASHRAE, Atlanta, GA, 1989

American Society of Heating, Refrigerating and Air Conditioning Engineers., "1993 Fundamentals Handbook," ASHRAE, Atlanta, GA, 1993

American Society of Heating, Refrigerating and Air Conditioning Engineers., "1995 Applications Handbook, Chapter 13 on Laboratory Systems" ASHRAE, Atlanta, GA, 1995

Anderson, S.A.,"Control Techniques for Zoned Pressurization," *ASHRAE Transactions,* Vol. 93,

Pt. 2, 1987
Athienitis, A.K., M.Stylianou, and J.Shou., "A Methodology for Building Thermal Dynamics Studies and Control Applications," *ASHRAE Transactions*, 1990
Bekker, J.E., Meckl, P.H., and Hittle, D.C., "A Tuning Method for First- Order Processes with PI Controllers," ASHRAE Transactions, 1991
Bell and Gossett, "Hydronic Systems Engineering Manual," *Bell & Gossett, ITT Fluid Handling Division*, Morton Grove, Illinois, 1964
Braun, J.E., J.W. Mitchell, S.A.Klein, and W.A.Beckman., "Performance and Control Characteristics of a Large Cooling System,"*ASHRAE Transactions*, Vol. 93, Pt.1, 1987
Borresen, B.A., "HVAC Control Process Simulation," *ASHRAE Transactions*, 1981
Dorf, R.C., "Modern Control Systems," *Addison-Wesley Publishing Company*, Reading, MA, 1980
Hitchings, D.T., "Laboratory Space Pressurization Control Systems," *ASHRAE Journal*, February, 1994
Haines, R.W., and D.C. Hittle., "Control Systems for Heating, Ventilating, and Air-Conditioning," Van Nostrand Reinhold, New York, 1983
Incropera, F.P., and D.P.Dewitt., "Introduction to Heat Transfer," *John Wiley & Sons*., New York, 1985
Kays, W.M., and A.L. London., "Compact Heat Exchangers," *McGraw-Hill Book Company*, New York, 1964
Klein, S.A., and F.L. Alvarado., "Engineering Equation Solver," *F-Chart Software*, Middleton, WI, 1997
Li, X.M., and W.J.Wepfer., "Recursive Estimation Methods Applied to a Single-Zone HVAC System," *ASHRAE Transactions*, 1987
Marsh C.W., " DDC Systems for Pressurization, Fume hood Face Velocity and Temperature Control in Variable Air Volume Laboratories," *ASHRAE Transactions*, Vol.94, Pt.2, 1988
Mehta, D.P., "Dynamic Performance of PI Controllers: Experimental Validation," *ASHRAE Transactions*, 1987
Mollenkamp, R.A., "Modern Digital and Automatic Process Control," *McGraw-Hill Chemical Engineering Seminar*, McGraw-Hill, New York, 1981
Neuman, V.A., and H.M.Guven., " Laboratory Building HVAC Systems Optimization," *ASHRAE Transactions*, Vol. 94., Pt. 2., 1988
Neuman, V.A., "Design Considerations for Laboratory HVAC Systems Dynamics," *ASHRAE Transactions*, Vol.95, Pt.1., 1989.
Park, C., S.T. Bushby., and G.E. Kelly., "Simulation of a Large Building System Using the HVACSIM+ program," *ASHRAE Transactions*, Part. 1, Vol. 95, 1989
Pearson, J.T., R.G. Leonard., and R.D. McCutchan., "Gain and time constant for finned serpentine crossflow heat exchangers," *ASHRAE Transactions*, Vol. 80, Pt.2,1974
Shah, M.M., "Estimated Rate of Pressurization and Depressurization of Buildings," *ASHRAE Transactions*, Vol.86, Pt.1, 1980
U.S. Dept. of Commerce., "HVACSIM+ Building Systems and Equipment Simulation Program Reference Manual," *NBSIR 84-2996*, National Bureau of Standards, Washington, 1984
Zaheer-uddin, M., and G.R.Zheng., "A Dynamic Model of a Multizone VAV System for Control Analysis," ASHRAE Transactions, Vol. 100, Pt.1, 1994

NOMENCLATURE:

a	authority	
A	Area	m^2

c_v	Specific heat at constant volume	kJ/kg.K
c_p	Specific heat at constant pressure	kJ/kg.K
C	Capacitance	kJ/kg.K
cfm	cubic feet per minute	
d_t	delay time	
e	Error in PID algorithm	
h	Enthalpy	kJ/kg
hc	Convection coefficient	W/(m^2.K)
I_g	Integral gain in PID algorithm	
k	Thermal conductance	W/(m.K)
K	Friction coefficient	
K_l	Envelope leakage constant	
K_o	Frictional coefficient when damper or valve is fully open	
L	Length	m
Δl	Wall thickness	m
m	Mass	kg
$\dot{m}$	Rate of mass flow	kg/sec.
NTU	Number of transfer units	
n	Flow exponent	
P	Pressure	kPa
ΔP	Pressure differential	kPa
P_g	Proportional gain in PID algorithm	
$\dot{q}_{gen}$	The rate of generation of internal heat	kJ/min
$\dot{q}_{load}$	Room thermal load	kJ/min
$\dot{q}_{tr}$	Rate of heat transfer by conduction	kJ/min
r_a	Command actuator position	
R	Gas constant	kJ/kg.K
Rt	Thermal resistance	m^2.K/W
S_t	Sample time	seconds
S_g	System gain	
t	time	seconds
Tau	Mass-capacitance	W-sec/K
t_o	Dead time	seconds
T	Temperature	^oC
u	Specific internal energy	kJ/kg
U	Total internal energy	kJ
UO	Overall heat transfer coefficient	W/(m^2.K)
V	Volume	m^3

$\dot{v}$	Volumetric flow rate	m^3/min
W_f	damper parameter	
x	Space coordinate to indicate the direction of heat flow	

Greek symbols:

ε	Coil effectiveness	
α	Thermal diffusivity	m^2/s, ft^2/s
λ	Damper leakage constant	
μ	Damper parameter	
ρ	Density	kg/m^3
τ	Time constant	seconds

Subscript:

a	Air
act	Actuator
ad	Adjacent space
cl	Ceiling
coil	Coil
dfo	Damper fully open
e	Exhaust
ex	General exhaust
f	Fluid (water)
fh	Fume hood
fl	Floor
gen	Generation
i	In
max	Maximum
min	Minimum
o	Out
p	Constant pressure
pw	Panel wall
r	Room
s	Supply
sp	Setpoint
ss	Steady state
st	Thermostat
v	Constant volume
w	Wall surface

APPENDIX:

Table 1

List of Simulation Parameters and Fixed Variables

Name	Symbol	Value
		SI
Envelope leakage constant	K	1165.79 $\frac{L/sec.}{(kPa)^n}$
Flow exponent	n	0.65
Supply pressure	P_S	101.526 (kPa)
Adj. space pressure	P_{ad}	101.526 (kPa)
Adj. space temperature	T_{ad}	21 (^oC)
Overall heat transfer coefficient between adjacent space and the wall surface	$U_{w,ad}$	1.70 ($\frac{W}{m^2 - ^oC}$)
Equivalent thermal capacitance	Tau_w	9489.31 ($\frac{kJ}{^oK}$)
Connective heat transfer coeff. between room and the wall surface	$hc_{r,w}$	8.29 $\frac{W}{m^2 - ^oC}$

Table 2

Damper Simulation Parameters

λ = 1.0e(-6); W_f = 1.0; K_{34}= 3.12 e(-7); K_0= 31.54;

Authority	K_{12} (" kPa/(L/sec)^2.0)	Maximum $\dot{v}_s$ (L/s)
1.00	-3.12e-7	1084
.70	1.72e-5	908
.50	4.05e-5	767
.20	1.63e-4	485
.10	3.67e-4	343
.05	7.75e(-4)	243
.01	4.04e(-3)	109

Table 3
Controller Gains

Control sequence	Control component	Pg (signal/error)	IgSt (signal/error)
Pressure	Supply damper	0.188	.061
Heating	Supply damper	.00018	6.1e(-5)
	General exhaust	.3675	.163
Cooling w/o load	Supply damper	.00018	6.1 e(-5)
	Coil valve	.00735	.00583
Cooling with load	Supply damper	3.0 e(-6)	2.5 e(-5)
	Coil valve	1.04	.00780

Table 4
List of coil simulation parameters

Description	Symbol	Equation used	Values
Max. supply air temp	$T_{a,o\|}$		22.22 ^oC
Max. supply air flow[1,2]	$\dot{v}_{s\|\max}$		943.8 L/s
Coil entering air temp.[3]	$T_{a,I}$		12.78 ^oC
Max. design coil heat transfer	$\dot{q}_{\max}$	$\dot{q}_{\max} = 1.08\ \dot{v}_{s\|\max}\ \Delta T_{a,\max}$ $\Delta T_{a,\max} = (T_{a,o\|\max} - T_{a,i})$	10,551 W
Max. coil water flow rate	$\dot{v}_{f\|\max}$	$\dot{v}_{f\|\max} = \frac{\dot{q}_{\max}}{500 \Delta T_f}$	.220 L/s
Design water side temp. drop[4]	ΔT_f		11.11 ^oC
Air mass- capacitance	C_a	$C_a = \dot{v}_{s\|\max} \rho_a C_{p,a}$	6.83 $\frac{Btu}{min - ^oF}$
Water mass- capacitance	C_f	$C_f = \dot{v}_{f\|\max} \rho_f C_{p,f}$	5.31 $\frac{Btu}{min - ^oF}$
Ratio of fluid heat capacity	C_r	$C_r = \frac{C_{min}}{C_{max}} = \frac{C_w}{C_a}$	0.777
Effectiveness[5]	ε		0.70
Overall coil heat transfer coefficient[6]	UA	$\varepsilon = f(NTU, \frac{C_{min}}{C_{max}})$	13.28 $\frac{Btu}{min - ^oF}$

1. Sufficient value at max. ventilation 2. Based on maximum fume hood exhaust
3. Design condition 4. Good design value (Bell & Gossett 1977) 5. Assumed value
6. Using ε plot